

Conformation-dependent Photostability among and within Single Conjugated Polymers

Heungman Park[†], Dat Tien Hoang[†], Keewook Paeng^{†‡}, Jaesung Yang[†], Laura J. Kaufman^{†*}

[†]Department of Chemistry, Columbia University, New York, NY 10027, USA

[‡]Department of Chemistry, Sungkyunkwan University, Suwon 440-746, Republic of Korea.

*Corresponding author: kaufman@chem.columbia.edu

Supporting Information

1. Supporting Materials and Methods

A. MEH-PPV synthesis

MEH-PPV was synthesized as described previously.¹ The MEH-PPV had $M_w = 168$ kDa with PDI = 2.1 with a single-peak trace measured by gel-permeation chromatography. MEH-PPV was diluted in 4.4 and 3.1 wt% polystyrene (PS, Polymer Source, MW = 6.4 kDa, PDI = 1.05) with either toluene or chloroform as the solvent. These solutions were spin-coated at 2000 rpm onto native oxide covered silicon wafers resulting in ~ 200 nm thick films as measured via atomic force microscopy.

B. Photobleaching experiment with a compact fluorescent lamp

Three samples were prepared from an MEH-PPV/PS chloroform solution. A control sample was covered with aluminum foil to prevent photobleaching. The samples were illuminated with a 23 W commercial compact fluorescent lamp in air as shown in Fig. S1.

C. Photobleaching experiment with a laser and M measurements

Experiments were performed on a home-built wide-field epi-fluorescence microscope equipped with a vacuum cryostat (Janis, ST-500). Samples were placed in vacuum at ~ 1 mTorr for 1 hour before laser beam illumination for bleaching experiments and M measurements. Excitation light at 532 nm (Spectra Physics; Millennia Vs, Nd:Vanadate 532 nm diode laser) was employed. A quarter waveplate was used to create circularly polarized light. The beam was coupled into a multimode fiber (Newport, F-MCB-T-1FC), which was shaken mechanically to eliminate speckles and homogeneously illuminate the field of view. M measurements were performed by rotating a linear polarizer placed before the objective lens (Zeiss, LD Plan-Neofluar, air 63x, NA = 0.75, WD = 1.5 mm) at a rate of 10 °/s such that each M measurement took 36 s. Excitation light was 5 mW (~50 W/cm²) at the sample, with intensity variations of $\pm 2\%$ as a function of polarization angle, primarily due to imperfect optics alignment. The polarization extinction ratio after the objective varied from 41:1 to 151:1 depending on the polarization of the beam.

The fluorescence was collected by the same objective lens and passed through a dichroic mirror followed by a long-pass filter. The emitted light was imaged onto an electron multiplying charge-coupled device camera (Andor iXon DV887; EMCCD). We verified that imperfect polarization conditions employed did not significantly affect M measurements by measuring M distributions from pPDI (N,N-bis(3-phosphonopropyl)-3,4,9,10-perylene dicarboximide) dye molecules, which have a single transition dipole and are thus expected to have $M = 1$. Almost all measured M values were between 0.9 and 1.1.

Following an M measurement on MEH-PPV polymers, the polarizer was removed and a 60 mW (~ 600 W/cm²) isotropic beam was used to illuminate the same sample area to partially photobleach the MEH-PPV molecules for 200 s. Following this, the polarizer was replaced and excitation M measurements were repeated with the same M measurement conditions. Finally, the same sample spot was illuminated with an isotropic 80 mW (~ 800 W/cm²) beam for 400 s to further bleach the MEH-PPV molecules. During the M measurements and the photobleaching periods, movies were collected continuously at a frame rate of 5 Hz. Typically, 3 - 5 movies each with ~ 100 molecules combined for each data set presented.

D. Data analysis

Data was analyzed using a custom computer program written in Python. Bright features were identified by the Crocker–Grier algorithm implemented in Python.^{2, 3} Molecules exhibiting photoblinking during M measurements or complete photobleaching during either M or the intensity measurement following the first M measurement were excluded. Each retained feature and background intensity were calculated from the center 7 by 7 pixel area and the 9 by 9 pixel area as shown in Fig. S2. Feature intensity was defined as the mean value of the brightest five pixels among the central 49 pixels. Intensity was defined by this method rather than by integrating all intensities to allow for straightforward comparison between feature intensity and background pixel intensity. Using 7 by 7 pixels ensures that slight mismatch (typically 1-2 pixels) between the actual center of each feature and the center position located by the algorithm does not affect the feature intensity calculation. Background intensity was obtained in the same way, considering the 32 pixels in the 9 x 9 area that are not a part of the 7 x 7 feature area. To assure statistically equivalent consideration for background and feature calculation, an additional 17 pixels adjacent to the 9 x 9 area were used to provide 49 pixels for the background intensity calculation. Background subtracted frame-by-frame (angle-by-angle) center feature intensity trajectories were used to determine M values by fitting the data to Eq. 1. While M varies between 0 and 1 by definition, some M values from experimental data are greater than 1 due to noise.

E. Sample data

Fig. S4 shows data from a typical molecule from which an M measurement, intensity/partial photobleaching trace, second M measurement, and second intensity/photobleaching trace was collected. Initially the molecule displayed the relatively low M value of 0.31. During the first application of higher intensity light, the intensity trajectory showed complex behavior, with an initially abrupt decay followed by a small increase in intensity and then a slower continuous intensity decrease. Continuous, rather than step-wise, fluorescence intensity decays in

conjugated polymers have been attributed to the presence of a relatively large number of emitting chromophores exhibiting serial photobleaching.⁴⁻⁸ The modulation depth measured following partial photobleaching revealed a higher M value for this molecule than before exposure to the moderate intensity light. The fluorescence intensity measurement following the second polarization modulation measurement also revealed complex, largely continuous bleaching behavior, suggestive of the continued presence of multiple absorbing and emitting chromophores.

F. Detailed simulated photobleaching procedure

Each transition dipole was assigned a random number (P_{random}) between 0 and 1, and all transition dipoles assigned a number below a given value, termed the bleaching probability (P_{bleach}), were removed before recalculation of M. For example, if a transition dipole was assigned $P_{\text{random}} = 0.6$ for a simulation with $P_{\text{bleach}} = 0.7$, the transition dipole was excluded. The simulated 2D photobleaching was performed with P_{bleach} set so as to result in an intensity change similar to that seen experimentally. Fig. S7a shows a 2D FJC simulated photobleaching experiment. There is an obvious shift in the M distribution toward higher M values due to statistical effects associated with decreasing number of transition dipoles upon partial photobleaching. The photobleaching simulation was also generalized to 3D (Fig. S7c). As in the 2D simulations, each transition dipole was assigned a random number, and the simulation was assigned a maximum bleaching probability ($P_{\text{bleach,max}}$). In this case, $P_{\text{bleach,max}}$ represented an upper bound on the probability that a transition dipole would bleach, and actual likelihood of bleaching was set proportional to the square of the projection of the transition dipole onto the sample plane, expressed as $P_{\text{bleach}} = P_{\text{bleach,max}} \times \cos^2(\psi)$, where ψ is the angle between the transition dipole and the sample plane. If the maximum bleaching probability ($P_{\text{bleach,max}}$) was set at 0.7, a transition dipole's P_{random} was 0.6, and ψ was 0 degrees, i.e. $P_{\text{bleach}} = 0.7 \times \cos^2(0^\circ) = 0.7$, the transition dipole would be excluded upon recalculation of M. If ψ was 45 degrees, i.e. $P_{\text{bleach}} = 0.7 \times \cos^2(45^\circ) = 0.35$, the transition dipole would not be excluded because P_{random} was greater than P_{bleach} . To achieve the ~ 55% decrease in intensity seen after partial photobleaching in the experimental measurement on molecules prepared from dissolution in chloroform, the maximum probability of photobleaching was set at 70% in the 3D simulations. Fig. S7 shows M distributions for an ensemble of polymers composed of 15 transition dipoles before and after partial photobleaching in the 2D and 3D FJC models. In both cases, the partial photobleaching of random transition dipoles leads to an increase of M due to statistical effects, with no contribution from conformational differences, the generally accepted origin of differences in M values. Similar results are also shown in the FRC model (Fig. S9).

G. Noise effects

We assessed the effect of noise on M values near M = 1 because the average M decrease after partial photobleaching occurred only at high M values. Random Gaussian noise was added to a single simulated transition dipole in 3D as described by Eq. S1.

$$I(t) = I_0(t) + nI'(t)_{\text{Random}} \quad (\text{Eq. S1})$$

Because the calculation was performed on a single transition dipole, the noise-free M value is 1. As noise magnitude (n) increased, fitted M values increasingly deviated from 1; however this deviation was symmetric, and median M values remained at 1 at all noise levels. Three examples of simulated modulation intensity trajectories with different noise magnitude and corresponding M distributions over 10,000 simulations are shown in Fig. S10. This result shows that noise does not affect median M value, and change of M in molecules upon partial photobleaching is not due to changes in noise that occur with decreasing signal intensity and concomitant decrease in signal to noise.

Supporting Figures

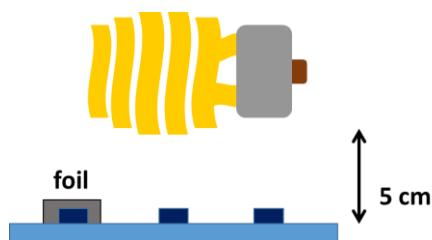


Figure S1. Schematic experimental diagram of photobleaching by a 23 W compact fluorescent lamp. The light intensity at the sample surface is approximately 10 mW/cm^2 .

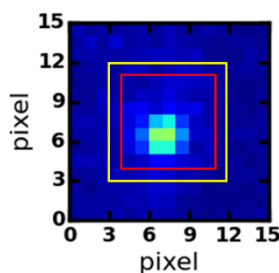


Figure S2. An image of a feature. Each feature was located by the Crocker–Grier algorithm. The feature intensity was calculated from the center 7 by 7 area (49 pixels inside the red box), and the background intensity was calculated from the pixels between the 9 by 9 area (yellow) and 7 by 7 area (yellow) with additional pixels added as described in the supporting text.

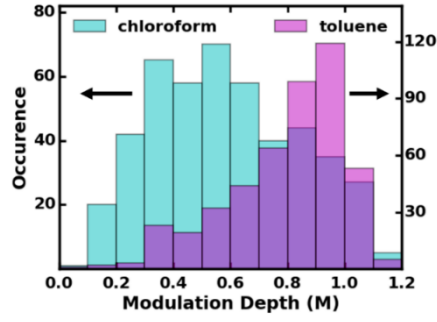


Figure S3. Excitation M distributions obtained from 466 MEH-PPV molecules prepared from dissolution in chloroform (cyan, left) and 472 MEH-PPV molecules prepared from dissolution in toluene (magenta, right) and immobilized in PS.

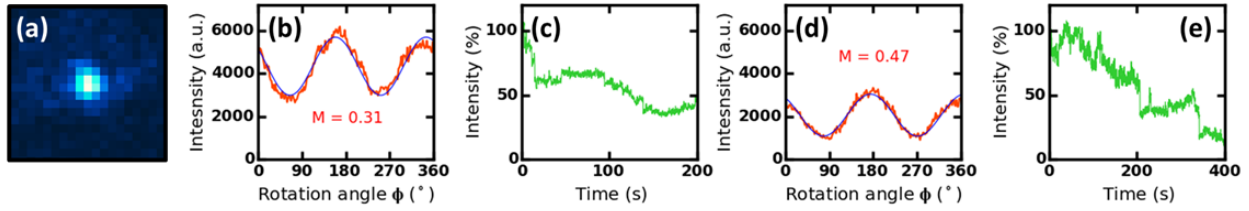


Figure S4. (a) Image of a single MEH-PPV feature prepared from chloroform, (b) M measurement before photobleaching, (c) intensity trajectory during the 1st photobleaching period, (d) M measurement after photobleaching, (e) intensity trajectory during the 2nd photobleaching period.

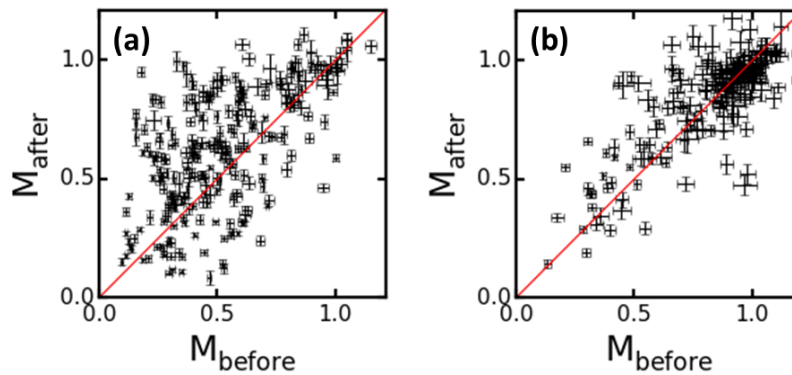


Figure S5. Scatter plots of M distributions before and after photobleaching MEH-PPV molecules prepared from dissolution in (a) chloroform and (b) toluene as also shown in Fig. 2 of the main text. The error bars are the fit uncertainties obtained from fitting the polarization modulation data to Eq. 1.

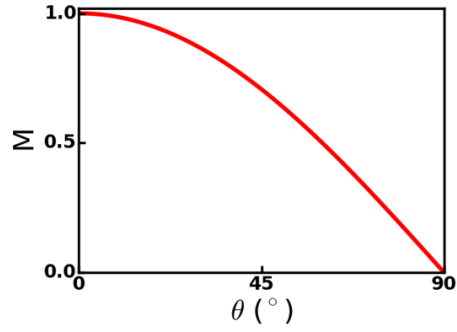


Figure S6. M of two transition dipoles on a 2D plane with respect to the angle between the two transition dipoles, θ . In this case, $M = \frac{1}{2}\sqrt{(1 + \cos 2\theta)^2 + (\sin 2\theta)^2}$.

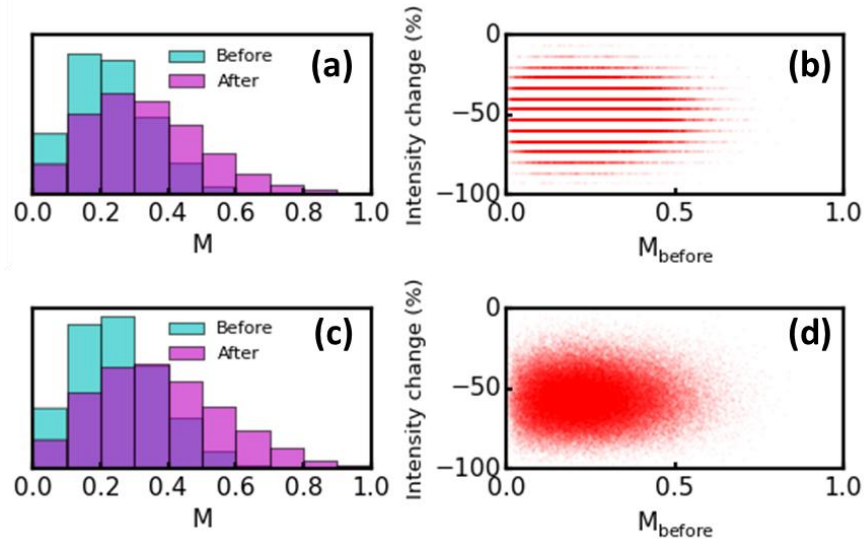


Figure S7. (a,b) 2D FJC model photobleaching simulation with $N = 15$ transition dipoles initially. Partial photobleaching was applied as described in the supporting text. Median $M = 0.22$ before bleaching and 0.32 after bleaching. (c,d) 3D FJC model photobleaching simulation with $N = 15$ transition dipoles initially. Median $M = 0.24$ before bleaching and 0.35 after bleaching. 100,000 polymers were generated in each simulation.

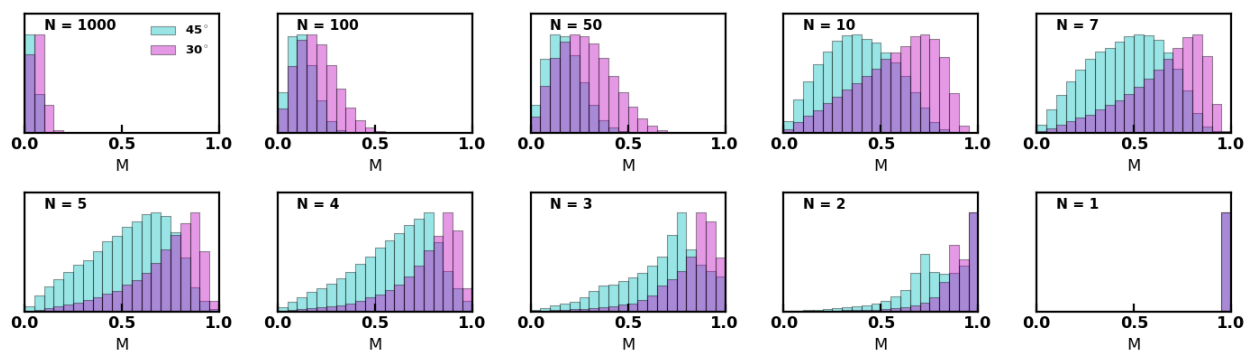


Figure S8. Monte Carlo simulation of M distributions within the 3D FRC model as a function of number (N) of transition dipoles with chain-to-chain angle of 45° (cyan) or 30° (magenta). 100,000 polymers were generated in each distribution.

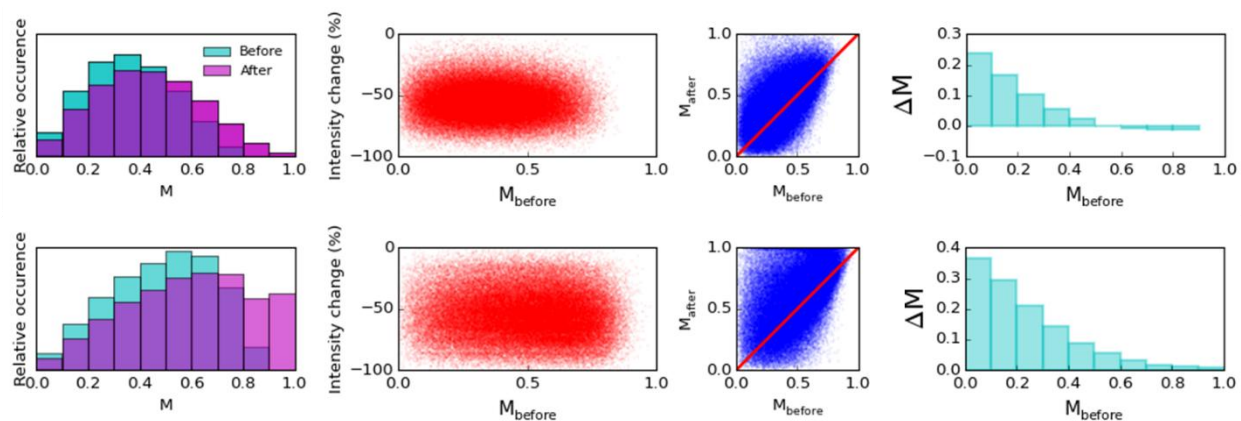


Figure S9. 3D FRC model simulations for (top) $N = 15$ and (bottom) $N = 8$ with 40° chain-to-chain angle and 70% maximum bleaching probability.

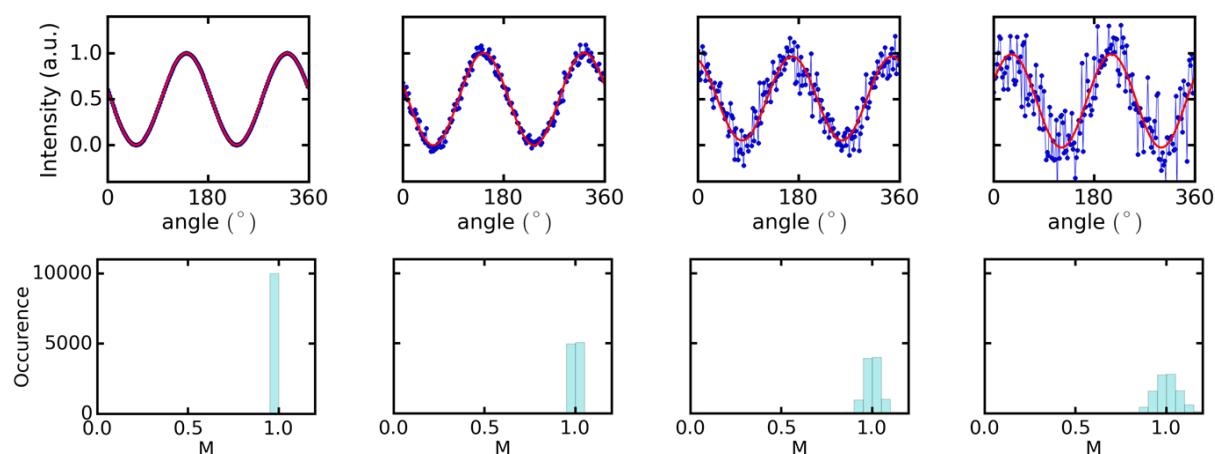


Figure S10. (top) Simulated intensity trajectories with noise as described in the supporting text and fits. (bottom) Corresponding M distributions with 10,000 simulated polymers as a function of increasing noise as described by Eq. S1.

References

1. Neef, C. J.; Ferraris, J. P. *Macromolecules* **2000**, 33, 2311-2314.
2. Crocker, J. C.; Grier, D. G. *Journal of Colloid and Interface Science* **1996**, 179, (1), 298-310.
3. An open source Python project: <https://github.com/soft-matter/trackpy>, 2015.
4. Huser, T.; Yan, M.; Rothberg, L. J. *Proc. Nat. Acad. Sci. - USA* **2000**, 97, 11187-11191.
5. Sarzi Sartori, S.; De Feyter, S.; Hofkens, J.; Van der Auweraer, M.; De Schryver, F.; Brunner, K.; Hofstraat, J. W. *Macromolecules* **2003**, 36, 500-507.
6. Liang, J.-J.; White, J.; Chen, Y.; Wang, C.; Hsiang, J.; Lim, T.; Sun, W.; Hsu, J.; Hsu, C.; Hayashi, M.; Fann, W.; Peng, K.; Chen, S. *Phys. Rev. B* **2006**, 74, 085209.
7. Traiphol, R.; Sanguansat, P.; Srihirin, T.; Kerdcharoen, T.; Osotchan, T. *Macromolecules* **2006**, 39, 1165-1172.
8. Ebihara, Y.; Vacha, M. *J. Phys. Chem. B* **2008**, 112, 12575-12578.